

Planar Hexacoordinate Silicon

Chen Chen,^a Meng-hui Wang,^a Sudip Pan^{*b} and Zhong-hua Cui,^{*a}

^aInstitute of Atomic and Molecular Physics, Key Laboratory of Physics and Technology for Advanced Batteries (Ministry of Education), Jilin University, Changchun, China

E-mail: zcui@jlu.edu.cn

^bFachbereich Chemie, Philipps-Universität Marburg, Hans-Meerwein-Strasse 4, 35032 Marburg, Germany

E-mail: pans@chemie.uni-marburg.de

Abstract

The occurrence of planar hexacoordination is very rare in cluster chemistry, particularly for main group elements. We report here a class of planar hexacoordinate silicon (phSi) in the global minimum isomer of SiE_3M_3^+ (E = N, P, As, Sb; M = Ca, Sr, Ba). Three Si-E multiple bonds between phSi and E centers is a key structural and electronic prerequisite for the observation of their perfect planarity and high stability. Especially, the electrostatic interactions between phSi and three M centers become less repulsive with decrease in electronegativity of E. Eventually, a sizable electrostatic attractive interaction exists in between phSi and M centers in $\text{SiSb}_3\text{M}_3^+$, leading to a true unprecedented phSi bonding motif which features three Si-Sb multiple bonds and three Si-M ionic bonds.

Introduction

Carbon plays the central role to develop the field of hypercoordination in cluster chemistry. Because of remarkable advancement in this field, now the present status could be fairly described as planar teracoordinate carbon (ptC)¹⁻²² is quite achievable (at least in paper), while planar pentacoordinate carbon (ppC)²³⁻²⁹ is a tougher target. But planar hexacoordinate carbon (phC) is an extraordinary and still almost unimaginable candidate. The long absence of examples of the latter category in the literature, despite huge advancement in both experimental techniques and computational approaches, supports this argument.

The search for phC was triggered by the report of a perfectly D_{6h} -symmetry CB_6^{2-} in 2000,³⁰ which was later turned out as a just local minimum, located at 30 kcal/mol above the lowest energy isomer.³¹ Then, it takes till 2012 to get the first genuine global minimum cluster having six connectivity with carbon in planar form in D_{3h} symmetric $CO_3Li_3^+$ cluster, although electrostatic repulsion between positively charged phC and Li centers and the absence of any significant orbital interaction between them make this hexacoordinate assignment questionable.³¹ In a recent study, Tiznado and Merino, and co-workers played with the combination in $CO_3Li_3^+$ cluster and finally succeeded to get a series of phC systems, $CE_3M_3^+$ (E = S, Se, Te; M = Li-Cs) where the natural charge on phC center is negative, and thus an electrostatic attraction exists between phC and positively charged alkali atoms.³² Note that the understanding of nature of electrostatic interaction based on point charges could be misleading as this is the electronic charge distribution that should be taken into account. This becomes obvious by looking at the electrostatic interaction between two neutral atoms such as in neutral N_2 . One would expect that the Coulomb interaction is very weak or slightly repulsive in nature, but it is actually highly attractive.³⁰ The authors in their study performed interacting quantum atoms (IQA) analysis,³¹⁻³⁴ which provides energy components for each individual bonds and it also gives attractive electrostatic interaction between phC and M centers. Therefore, in $CE_3M_3^+$ clusters phC is covalently bonded to three chalcogens and ionically connected to the three alkali metals. Since IUPAC definition³⁵ of coordination number does not demand orbital interaction, this is fair to call them phC systems.

Now, the question is whether we can also propose viable planar hexacoordinate silicon (phSi). In comparison to carbon, designing of its heavier homologues is more challenging task. This is because although due to the larger size the Steric repulsion between ligands decreases, the bonding strength of π and σ bonds between central atom and peripheral centers also greatly decreases. This is the reason why only a few limited numbers of ppSi and ppGe systems are reported so far.³⁶ Herein we made efforts to find the correct combination to get phSi system as the most stable isomer. Gratifyingly, we found a series of phSi as global minimum in SiE_3M_3^+ ($\text{E} = \text{N, P, As, Sb; M} = \text{Ca, Sr, Ba}$) clusters through a thorough potential energy surface (PES) exploration. However, the electrostatic interactions between phSi and three M centers are repulsive for $\text{E} = \text{N}$ and this repulsive nature gradually decreases with reduction in electronegativity of E. Eventually, it becomes attractive in nature in $\text{SiSb}_3\text{M}_3^+$ cluster.

Computational methods

The PES exploration of SiE_3M_3^+ ($\text{E} = \text{N, P, As, Sb; M} = \text{Ca, Sr, Ba}$) was performed using the particle swarm optimization (PSO) algorithm as implemented in the CALYPSO code.^{37,38} The random structures generated were initially optimized at the PBE0³⁹/def2-SVP level, and then further optimization followed by the harmonic vibrational frequency calculation of the low-lying energy isomers were done at the PBE0/def2-TZVP level. The energies were further refined with the single-point energy calculations for the low-lying energy isomers at the CCSD(T)⁴⁰/def2-TZVP//PBE0/def2-TZVP level. The T_1 diagnostic⁴¹ [ref] values are in a reasonable range, indicating that single-reference based method can be used with confidence (see supporting information). Total energies were corrected by the zero-point energies (ZPE) of PBE0. The BO-MD⁴² (Born–Oppenheimer molecular dynamics) simulations at 400 K were computed at the PBE0/def2-SVP level. The electronic analysis of global phSi was performed by the natural bond orbital (NBO)⁴³ and adaptive natural density partitioning (AdNDP)⁴⁴ analyses. The iso-chemical shielding surface (ICSS)⁴⁵ and the quantum theory of atoms in molecules (QTAIM)⁴⁶ analysis were carried out using the

Multiwfn program.⁴⁷ All these calculations above were performed using the GAUSSIAN 09 package.⁴⁸ The IQA⁴⁹ analysis was carried out using the ADF package.⁵⁰

Structures and stability

At the first step, we checked whether the D_{3h} symmetric phSi isomer of SiE_3M_3^+ (E = group 15 element, and M = group 2 element) is a minimum on the PES. The results in Figure S1 show that for E = Be and Mg, phSi isomer possesses a large out-of-plane imaginary frequency mode and thus they are discarded from further consideration. In case of $\text{SiBi}_3\text{M}_3^+$, even for M = Ca the phSi isomer possesses a small imaginary frequency. Although $\text{SiBi}_3\text{Sr}_3^+$ and $\text{SiBi}_3\text{Ba}_3^+$ are true minima, they are 2.2 and 2.5 kcal/mol higher in energy than the lowest energy isomer, respectively (Figure S2). Figure 1 displays some low-lying energy isomers of SiE_3M_3^+ (E = N, P, As, Sb; M = Ca, Sr, Ba) (see Figures S3-S6 for more isomers). For all the twelve cases, the most stable isomer is a D_{3h} symmetric phSi with $^1A_1'$ electronic state. The second lowest energy isomer, which is a ppSi, is located more than 49 kcal/mol above the phSi for E = N. The energy difference gradually decreases in moving from E = N to E = Sb. In case of $\text{SiSb}_3\text{M}_3^+$ the second lowest energy isomer is 4.6-6.1 kcal/mol higher in energy than phSi. The nearest triplet state isomer is very higher in energy (24-53 kcal/mol) than the global minimum.

BO-MD simulations at 400 K taking $\text{SiE}_3\text{Ca}_3^+$ as case studies were also performed and the related results are displayed in Figure S7. All trajectories show no isomerization or other structural alterations during the simulation time as indicated by small periodic RMSD values (root mean square deviation). This suggests that the global phSi SiE_3M_3^+ clusters also have reasonable kinetic stability against isomerization.

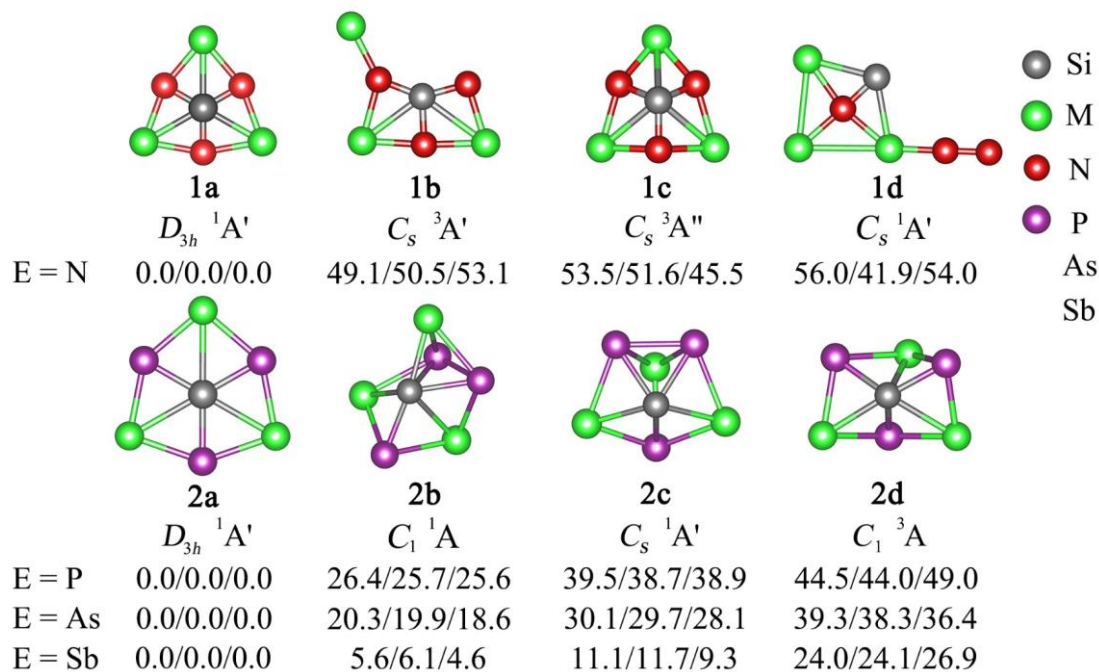


Figure 1. The structures and relative energies in kcal/mol of the low-lying energy isomers of SiE_3M_3^+ (E=N, P, As, Sb; M=Ca, Sr, Ba) obtained at the single-point CCSD(T)/def2-TZVP//PBE0/def2-TZVP calculations followed by the zero-energy correction of PBE0, the values from left to right refer to Ca, Sr, and Ba in sequence. The group symmetries and spectroscopic states are given.

The bond distances, natural partial charges and Wiberg bond indices (WBIs) for $\text{SiE}_3\text{Ca}_3^+$ are given in Table 1 (see Tables S1 and S2 for M = Sr, Ba). The Si-E bond distances are shorter than typical Si-E single bond distance computed using the self-consistent covalent radii proposed by Pyykkö,⁵¹ whereas the Si-M bond distance is almost equal to the Si-M single bond. The WBI values for the Si-E bonds lie within 1.1-1.3, while the same for Si-M bonds is almost negligible (0.02-0.04). This indicates partial double bond character in Si-E bonds and very little covalent character in Si-M bonds.

Table 1. Bond properties (B, distances in Å and WBIs in parenthesis) and NPA charges (Q, |e|) of $\text{SiE}_3\text{Ca}_3^+$ (E = N, P, As, Sb) computed at the PBE0/def2-TZVP level.

	$B_{\text{Si-E}}$	$B_{\text{Si-Ca}}$	$B_{\text{E-Ca}}$	Q_{Si}	Q_{E}	Q_{Ca}
E = N	1.669 (1.14)	2.555 (0.02)	2.246 (0.22)	1.57	-1.93	1.74
E = P	2.180 (1.34)	2.935 (0.03)	2.640 (0.27)	0.25	-1.42	1.67
E = As	2.301 (1.33)	3.004 (0.03)	2.721 (0.29)	0.07	-1.34	1.65
E = Sb	2.538 (1.29)	3.155 (0.04)	2.896 (0.30)	-0.39	-1.16	1.62

The bonding pattern of phSi was uncovered by the AdNDP⁴⁴ (adaptive nature density partitioning) analysis. As shown in Figure 2, the AdNDP bonds can be divided in three parts. First, in the first row, the six 1c-2e bonds (one center-two electrons) with occupation number (ON) of 1.71~1.94 are the s/p lone pairs of E atoms (E=N, P, As, Sb). The three Si-E 2c-2e σ bonds (ON=ca. 2.0) is also given in the first row. The 4c-2e π bonds of the second row can be attributed to three π bonds that mainly locate at the SiE₃ region, thus combining with Si-E 2c-2e σ bonds reveal that the Si-E bonds possesses a clear multiple bonding characteristic, being consistent with the bonding properties discussed above. These Si-E multiple bonds pattern vividly follows our π -localization strategy, where the SiE₃ motifs having a firm π -localized framework provides a driving force for the title phSi planarity and stability.

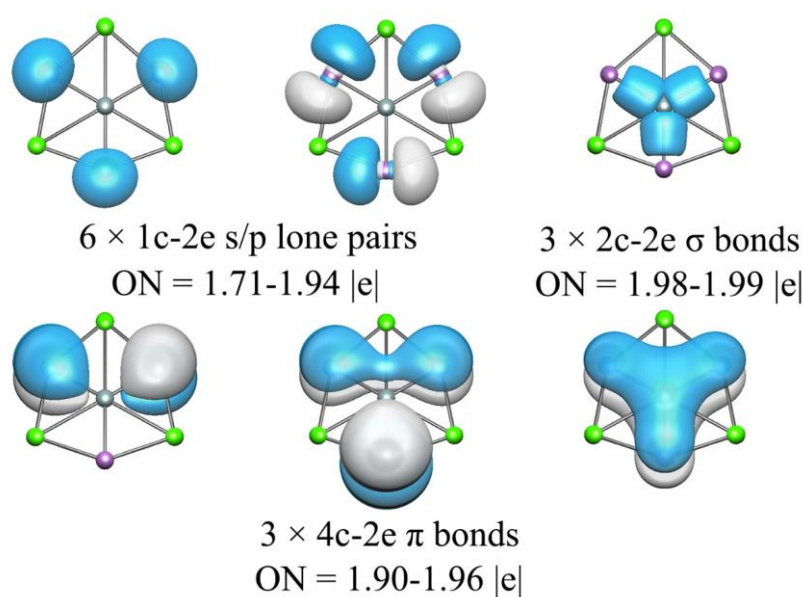


Figure 2. AdNDP bonds and their occupation numbers (ONs) in |e| of SiE₃Ca₃⁺ (E = N,

P, As, Sb) obtained at the PBE0/def2-TZVP level.

To understand the electronic properties of phSi, the natural bonding orbital (NBO)⁴³ analysis was performed at the PBE0/def2-TZVP level. As shown in Table 1, the natural population analysis (NPA)⁵² charges suggest that the strong charge transfer from the peripheral M ligands to SiE₃ motifs occurs in all phSi species, indicated by that the M^{δ+} with ca. +1.7 |e| but E possesses the large negative charges (-1.2~-1.9 |e|). Such charge distribution reveals that the strong electrostatic attraction accounts for the short E-M contacts, meanwhile, where the bridging E^{δ-} is responsible for the Si-M short contacts. For the SiE₃ motifs, the phSi center has a large positive NPA charge (+1.57 |e|) in SiN₃Ca₃⁺, but it decreases sharply as it goes from E=N to Sb of SiE₃Ca₃⁺. Especially, phSi carries a considerable negative charge (-0.39 |e|) in SiSb₃Ca₃⁺. Thus, the electrostatic interactions between phSi center and three M ligands become less repulsive along with the less electronegative E, and eventually turn into electrostatic attractive occurs in SiSb₃M₃⁺, making a true planar hexacoordinate silicon bonding. Such electrostatic interaction change behavior is similar to CE₃Li₃⁺ (E=group 16 elements) where electrostatic interactions between phC and Li gradually become less repulsive along with the less electronegative E, and even turn into electrostatic attraction in global CSe₃Li₃⁺ and CTe₃Li₃⁺ clusters.⁵³ It is worthy of noting that the M ligands is clearly coordinated to phSi or phC although the M-C (phC) or M-Si (phSi) present the electrostatic repulsion according to the coordination definition of IUPAC, where “the coordination number of a specified atom in a chemical species as the number of other atoms directly linked to that specified atom”.⁵⁴ Nevertheless, the phSi in SiSb₃Ca₃⁺ and phC in CSe₃Li₃⁺ and CTe₃Li₃⁺⁵³ can be verified to be a true planar hexacoordinate silicon/carbon bonding involving three C(Si)-E multiple bonds and three C(Si)-M ionic bonds.

The interacting quantum atoms (IQA)⁴⁹ analysis was considered herein for understanding the inter-atomic interaction energy (V_{Total}), which can be evaluated and decomposed into electrostatic (ionic, V_{Ionic}) and exchange (covalent, V_{Coval}) contributions. The former is classical electrostatic terms, yet the latter is based on the

exchange-correlation part of the electron-electron interaction. The three SiE_3M_3^+ ($\text{M}=\text{Ca}, \text{Sr}, \text{Ba}$) present an essentially identical behavior of the IQA analysis, thus only $\text{SiE}_3\text{Ca}_3^+$ is given in Table 2 and the other two can be found in Table S3 and S4. As shown in Table 2, the IQA energy decomposition analysis confirms our electronic analysis above. Noteworthy, the Si-Ca inter-atomic interaction displays a repulsion (509.8 kcal/mol) in $\text{SiN}_3\text{Ca}_3^+$ and it sharply decreases in the heavier $\text{SiE}_3\text{Ca}_3^+$ species, and even become attractive in $\text{SiSb}_3\text{Ca}_3^+$, which fully agrees with the results originated from NPA charges distribution in $\text{SiSb}_3\text{Ca}_3^+$, suggesting a true planar hexacoordinate silicon bonding. The Si-N of $\text{SiN}_3\text{Ca}_3^+$ possesses a big interaction energy (V_{Total}) of -1232.1 kcal/mol, and it decreases sharply in the heavier $\text{SiE}_3\text{Ca}_3^+$ ($\text{E}=\text{P}, \text{As}, \text{Sb}$) analogues (-450.7 ~ -118.9 kcal/mol), yet the covalent contribution V_{Coval} is gradually enhanced. The similar decreasing behavior from $\text{E}=\text{N}$ to heavier species also occurs in the E-Ca ligand-ligand interactions (from -476.4 to -185.4 kcal/mol), yet it is essentially ionic. The E-M ligand-ligand stabilizing interactions in all phSi species provide an important driving force between phSi center and M ligands, especially in the SiE_3M_3^+ ($\text{E}=\text{N}, \text{P}, \text{As}$) cases having a clear electrostatic repulsion. Overall, the D_{3h} -symmetry global phSi cluster is stabilized significantly by the three M ligands with additional electrostatic stabilization via the strong charge transfer from M to the SiE_3 moiety. Thus, both the Si-E multiple bonds and electrostatic interactions between M ligands to SiE_3 make the phSi SiE_3M_3^+ a highly thermodynamically and kinetically stable species.

Table 2. Energy components of interacting quantum atoms (IQA) analysis in kcal/mol for the D_{3h} -symmetric phSi $\text{SiE}_3\text{Ca}_3^+$ ($\text{E} = \text{N}, \text{P}, \text{As}, \text{Sb}$) systems, where inter-atomic interaction energy (V_{Total}) can be evaluated and decomposed into electrostatic (ionic, V_{Ionic}) and exchange (covalent, V_{Coval}) contributions.

$\text{SiE}_3\text{Ca}_3^+$	$\text{SiN}_3\text{Ca}_3^+$	$\text{SiP}_3\text{Ca}_3^+$	$\text{SiAs}_3\text{Ca}_3^+$	$\text{SiSb}_3\text{Ca}_3^+$
$V_{\text{Total}}(\text{Si-E})$	-1232.1	-450.7	-247.6	-118.9
$V_{\text{Ionic}}(\text{Si-E})$	-1117.6	-303.5	-95.1	25.2
$V_{\text{Coval.}}(\text{Si-E})$	-114.5	-147.1	-152.5	-144.1
$V_{\text{Total}}(\text{Si-Ca})$	509.8	194.7	80.7	-40.2
$V_{\text{Ionic}}(\text{Si-Ca})$	515.2	202.9	90.6	-28.6

$V_{\text{Coval.}}(\text{Si-Ca})$	-5.5	-8.2	-10.0	-11.6
$V_{\text{Total}}(\text{E-Ca})$	-476.4	-303.9	-252.7	-185.4
$V_{\text{Ionic}}(\text{E-Ca})$	-413.1	-249.8	-201.6	-136.1
$V_{\text{Coval.}}(\text{E-Ca})$	-63.3	-54.1	-51.1	-49.4

The bonding pattern and electronic properties of the title phSi based on π -localization strategy is clearly different from the planar species using the π -delocalization strategy,⁴ where the latter possesses the balance but weak planar center-ligand bonds, yet the strong covalent bonds occur in the former cases. Beside bonding pattern, the planar hypercoordinate center possesses a different picture, the valence population (VP) of the title phSi atom in $\text{SiE}_3\text{Ca}_3^+$ is $3s^{0.59\sim 1.35}3p_x^{0.53\sim 1.00}3p_y^{0.53\sim 1.00}3p_z^{0.63\sim 0.95}$, where 3s and 3p occupancies gradually increase as it goes from E=N to E=Sb (see Table S5). However, these occupancies are significantly lower than the prototype π -delocalization ptC, for example, CAI_4^{2-} ($2s^{1.62}2p_x^{1.77}2p_y^{1.77}2p_z^{1.61}$).^{4,21} Such low valence occupancies are due to the strong charge transfer from phSi center to ligand E, yet the strong Si-E multiple bonds make phSi center a considerable total WBI value (3.5~4.1).

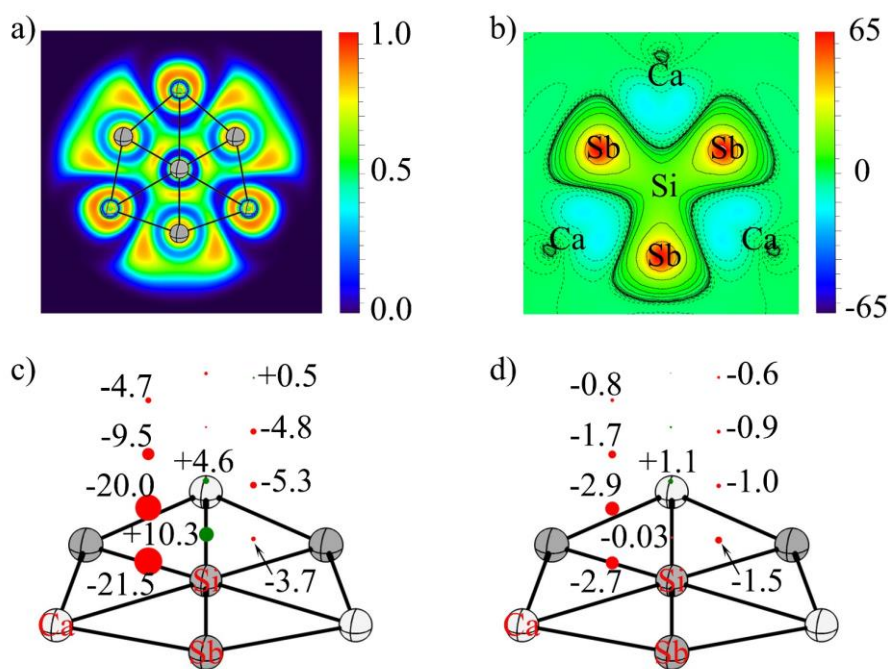


Figure 3. a) ELF, b) ICSS_{zz}, c) NICS_{zz}, and d) NICS_{zz} (π orbitals) for $\text{SiSb}_3\text{Ca}_3^+$. In d)

the diatropic and paratropic tensors are shown in red and green, respectively. NICS values are in ppm All the cases see Figure S8.

In contrast to the pronounced aromaticity because of π delocalization,⁴ the essential feature in π -localized planar species is that π electrons mainly localize at strong covalent bonds rather than delocalize the whole plane, eventually leading to a relatively weak aromaticity. In details, the aromaticity character of the title phSi clusters is uncovered by the iso-chemical shielding surface (ICSS)⁴⁵ that is the isosurface of the nucleus-independent chemical shift (NICS) and presents an exceedingly intuitive picture on aromaticity. The ICSS_{zz}(1) (a z-direction component of ICSS_{zz} at 1.0 Å above) is displayed at Figure 3b and Figure S8. The phSi SiE₃Ca₃⁺ clearly displays a weak aromaticity for the whole plane, featuring a sharp change from Si-E bonds to the neighboring region, indicating -20.0 ppm at Si-Sb region to +4.6 ppm (Si-Ca) and -5.3 ppm (Sb-Si-C triangle) as given Figure 3c. The canonical molecular orbital (CMO) dissection into π orbitals of NICS_{zz} grid is given in Figure 3d, where NICS_{zz} (π electrons) is clearly smaller as compared to the total NICS_{zz}. Additionally, the strong electron localization within Si-E multiple bonds is also found in the electron localization function (ELF) picture in Figure 3a. Overall, the electronic analysis of phSi strongly revealed that strong Si-E multiple bonds rather than π electron delocalization give rise to the extraordinary stability of the title phSi cluster, effectively verifying the assessment of the π -localized strategy proposed herein.

Conclusions

In summary, the π -localized design approach is further extended here and results in the first global isolated planar hexacoordinate silicon. The twelve phSi clusters have been achieved in SiE₃M₃⁺, in which the Si-E multiple bonds and strong electrostatic interactions between ligand M and SiE₃ motifs are effectively formed, giving rise to the high stability and planarity of the title phSi species. The electrostatic interactions between phSi center and three M ligands become less repulsive along with the less electronegative E, and eventually turn into the firm electrostatic attractive in SiSb₃M₃⁺, making an unprecedented planar hexacoordinate silicon bonding associated with three

Si-Sb multiple bonds and three Si-M ionic bonds. The π -localization strategy not only breaks the limit of π -acceptor/ σ -donor ligands, but enriches the number of valence electron (usually 18 electrons) for designing planar species, as well as gives rise to a new insight on the chemical bonding and electronic properties of planar species.

Acknowledgments

This work was funded by the National Natural Science Foundation of China (No. 11922405, 11874178, 91961204). The partial calculations in this work supported by High Performance Computing Center of Jilin University, China.

Conflict of interest

The authors declare no conflict of interest.

References

- (1) Kekulé, A. Ueber die s. g. gepaarten Verbindungen und die Theorie der mehratomigen Radicale. *A. Ann. Chem. Pharm.* **1857**, 104, 129-150.
- (2) Van' t Hoff, J. H. Sur les formules de structure dans l'espace. *Arch. Neerl. Sci. Exactes Nat.* **1874**, 9, 445-454.
- (3) Le Bel, J. A. Sur le relation qui existant entre les formules atomiques des corps organiques, et le pouvoir rotatoire de leurs dissolutions. *Bull. Soc. Chim. Fr.* **1874**, 22, 337-347.
- (4) Hoffmann, R.; Alder, R. W.; Wilcox, C. F. Planar tetracoordinate carbon. *J. Am. Chem. Soc.* **1970**, 92, 4992-4993.
- (5) Boldyrev, A. I.; Simons, J. Tetracoordinated Planar Carbon in Pentaatomic Molecules. *J. Am. Chem. Soc.* **1998**, 120, 7967-7972.
- (6) Schleyer, P. v. R.; Boldyrev, A. I. A New, General Strategy for Achieving Planar Tetracoordinate Geometries for Carbon and other Second Row Periodic Elements. *J. Chem. Soc., Chem. Commun.* **1991**, 21, 1536-1538.
- (7) Sahin, Y.; Prasang, C.; Hofmann, M.; Subramanian, G.; Geiseler, G.; Massa, W.; Berndt, A. A Diboracyclopropane with a Planar Tetracoordinate Carbon Atom and a Triborabicyclobutane. *Angew. Chem., Int. Edit.* **2003**, 671-674.
- (8) Crans, D. C.; Snyder, J. P. Tetracoordinate planar carbon: a singlet biradical. *J. Am. Chem. Soc.* **1980**, 102, 7152-7154.
- (9) Zheng, H. F.; Xu, J.; Ding, Y. H. A sixteen-valence-electron carbon-group 13 family with global penta-atomic planar tetracoordinate carbon: an ionic strategy. *Phys. Chem. Chem. Phys.* **2020**, 22, 3975-3982.
- (10) Ravell, E.; Jalife, S.; Barroso, J.; Orozco-Ic, M.; Hernandez-Juarez, G.; Ortiz-Chi,

- F.; Pan, S.; Cabellos, J. L.; Merino, G. Structure and Bonding in CE_5^- (E=Al-Tl) Clusters: Planar Tetracoordinate Carbon versus Pentacoordinate Carbon. *Chem. - Asian. J.* **2018**, 13, 1467-1473.
- (11) Yanez, O.; Vasquez-Espinal, A.; Pino-Rios, R.; Ferraro, F.; Pan, S.; Osorio, E.; Merino, G.; Tiznado, W. Exploiting electronic strategies to stabilize a planar tetracoordinate carbon in cyclic aromatic hydrocarbons. *Chem. Commun.* **2017**, 53, 12112-12115.
- (12) Contreras, M.; Pan, S.; Orozco-Ic, M.; Cabellos, J. L.; Merino, G. $E_3M_3^+$ (E=C-Pb, M=Li-Cs) Clusters: The Smallest Molecular Stars. *Chemistry* **2017**, 23, 11430-11436.
- (13) Castro, A. C.; Audiffred, M.; Mercero, J. M.; Ugalde, J. M.; Méndez-Rojas, M. A.; Merino, G. Planar tetracoordinate carbon in CE_4^{2-} (E=Al-Tl) clusters. *Chem. Phys. Lett.* **2012**, 519-520, 29-33.
- (14) Cui, Z. H.; Contreras, M.; Ding, Y. H.; Merino, G. Planar tetracoordinate carbon versus planar tetracoordinate boron: the case of CB_4 and its cation. *J. Am. Chem. Soc.* **2011**, 133, 13228-13231.
- (15) Wu, Y. B.; Lu, H. G.; Li, S. D.; Wang, Z. X. Simplest Neutral Singlet C_2E_4 (E=Al, Ga, In, and Tl) Global Minima with Double Planar Tetracoordinate Carbons: Equivalence of C_2 Moieties in C_2E_4 to Carbon Centers in CA_4 and CA_5 . *J. Phys. Chem. A.* **2009**, 113, 3395-3402.
- (16) Pattath, D. P.; Méndez-Rojas, M. A.; Merino, G.; Vela, A.; Hoffmann, R. Planar Tetracoordinate Carbon in Extended Systems. *J. Am. Chem. Soc.* **2004**, 126, 15309-15315.
- (17) Merino, G.; Méndez-Rojas, M. A.; Beltraan, H. I.; Corminboeuf, C.; Heine, T.; Vela, A. Theoretical analysis of the smallest carbon cluster containing a planar tetracoordinate carbon. *J. Am. Chem. Soc.* **2004**, 126, 16160-16169.
- (18) Merino, G.; Méndez-Rojas, M. A.; Vela, A. $(C_5M_{2-n})^n$ (M=Li, Na, K, and n=0, 1, 2). A New Family of Molecules Containing Planar Tetracoordinate Carbons. *J. Am. Chem. Soc.* **2003**, 125, 6026-6027.
- (19) Xu, J.; Zhang, X.; Yu, S.; Ding, Y. H.; Bowen, K. H. Identifying the Hydrogenated Planar Tetracoordinate Carbon: A Combined Experimental and Theoretical Study of CA_4H and CA_4H^- . *J. Phys. Chem. Lett.* **2017**, 8, 2263-2267.
- (20) Li, X.; Zhai, H. J.; Wang, L. S. Photoelectron spectroscopy of pentaatomic tetracoordinate planar carbon molecules: CA_3Si^- and CA_3Ge^- . *Chem. Phys. Lett.* **2002**, 357, 415-419.
- (21) Li, X.; Zhang, H. F.; Wang, L. S.; Geske, G. D.; Boldyrev, A. I. Pentaatomic tetracoordinate planar carbon, $[CA_4]^{(2-)}$: A new structural unit and its salt complexes. *Angew. Chem., In. Ed.* **2000**, 39, 3630-3632.
- (22) Boldyrev, A. I.; Li, X.; Wang, L. S. Experimental observation of pentaatomic tetracoordinate planar Si- and Ge-containing molecules: MA_4^- and MA_4 . *Angew. Chem., In. Ed.* **2000**, 39, 3307-3310.
- (23) Li, X.; Wang, L. S.; Boldyrev, A. I.; Simons, J. Tetracoordinated planar carbon in the Al_4C^- anion. A combined photoelectron spectroscopy and ab initio study. *J. Am. Chem. Soc.* **1999**, 121, 6033-6038.

- (24) Yang, L. M.; Ganz, E.; Chen, Z. F.; Wang, Z. X.; Schleyer, P. v. R. Four Decades of the Chemistry of Planar Hypercoordinate Compounds. *Angew. Chem., In. Ed.* **2015**, *54*, 9468-9501.
- (25) Merino, G.; Mendez-Rojas, M. A.; Vela, A.; Heine, T. Recent advances in planar tetracoordinate carbon chemistry. *J. Comput. Chem.* **2007**, *28*, 362-372.
- (26) Keese, R. Carbon flatland: planar tetracoordinate carbon and fenestranes. *Chem. Rev.* **2006**, *106*, 4787-4808.
- (27) Siebert, W.; Gunale, A. Compounds containing a planar-tetracoordinate carbon atom as analogues of planar methane. *Chem. Soc. Rev.* **1999**, *28*, 367-371.
- (28) Erker, G. Using bent metallocenes for stabilizing unusual coordination geometries at carbon. *Chem. Soc. Rev.* **1999**, *28*, 307-314.
- (29) Pan, S.; Cabellos, J. L.; Orozco-Ic, M.; Chattaraj, P. K.; Zhao, L.; Merino, G. Planar pentacoordinate carbon in CGas^+ derivatives. *Phys. Chem. Chem. Phys.* **2018**, *20*, 12350-12355.
- (30) Krapp, A.; Bickelhaupt, F. M.; Frenking, G. Orbital overlap and chemical bonding. *Chem-Eur. J.* **2006**, *12*, 9196-9216.
- (31) Pendas, A. M.; Blanco, M. A.; Francisco, E. Two-electron integrations in the quantum theory of atoms in molecules. *J. Chem. Phys.* **2004**, *120*, 4581-4592.
- (32) Blanco, M. A.; Pendas, A. M.; Francisco, E. Interacting quantum atoms: A correlated energy decomposition scheme based on the Quantum Theory of Atoms in Molecules. *J. Chem. Theory. Comput.* **2005**, *1*, 1096-1109.
- (33) Pendas, A. M.; Francisco, E.; Blanco, M. A. Two-electron integrations in the quantum theory of atoms in molecules with correlated wave functions. *J. Comput. Chem.* **2005**, *26*, 344-351.
- (34) Pendas, A.; Blanco, M. A.; Francisco, E. Chemical fragments in real space: Definitions, properties, and energetic decompositions. *J. Comput. Chem.* **2007**, *28*, 161-184.
- (35) Muller, P. Glossary of terms used in physical organic chemistry (IUPAC Recommendations 1994). *Pure Appl. Chem.* **1994**, *66*, 1077-1184.
- (36) Wang, M. H.; Dong, X.; Cui, Z. H.; Orozco-Ic, M.; Ding, Y. H.; Barroso, J.; Merino, G. Planar pentacoordinate silicon and germanium atoms. *Chem. Commun.* **2020**, *56*, 13772-13775.
- (37) Wang, Y. C.; Lv, J.; Zhu, L.; Ma, Y. M. CALYPSO: A method for crystal structure prediction. *Comput. Phys. Commun.* **2012**, *183*, 2063-2070.
- (38) Lv, J.; Wang, Y. C.; Zhu, L.; Ma, Y. M. Particle-swarm structure prediction on clusters. *J. Chem. Phys.* **2012**, *137*, 084104.
- (39) Adamo, C.; Barone, V. Toward reliable density functional methods without adjustable parameters: The PBE0 model. *J. Chem. Phys.* **1999**, *110*, 6158-6170.
- (40) Purvis, G. D.; Bartlett, R. J. A full coupled-cluster singles and doubles model: The inclusion of disconnected triples. *J. Chem. Phys.* **1982**, *76*, 1910-1918.
- (41) J.Lee, T.; MartinHead-Gordon; P.Rendell, A. Investigation of a diagnostic for perturbation theory. Comparison to the T1 diagnostic of coupled-cluster theory. *Chem. Phys. Lett.* **1995**, *243*, 402-408.
- (42) Millam, J. M.; Bakken, V.; Chen, W.; Hase, W. L.; Schlegel, H. B. Ab initio

- classical trajectories on the Born-Oppenheimer surface: Hessian-based integrators using fifth-order polynomial and rational function fits. *J. Chem. Phys.* **1999**, 111, 3800-3805.
- (43) Foster, J. P.; Weinhold, F. Natural Hybrid Orbitals. *J. Am. Chem. Soc.* **1980**, 102, 7211-7218.
- (44) Zubarev, D. Y.; Boldyrev, A. I. Developing paradigms of chemical bonding: adaptive natural density partitioning. *Phys. Chem. Chem. Phys.* **2008**, 10, 5207-5217.
- (45) Chen, Z. F.; Wannere, C. S.; Corminboeuf, C.; Puchta, R.; Schleyer, P. v. R. Nucleus-independent chemical shifts (NICS) as an aromaticity criterion. *Chem. Rev.* **2005**, 105, 3842-3888.
- (46) Corts-Guzman, F.; Bader, R. F. W. Complementarity of QTAIM and MO theory in the study of bonding in donor-acceptor complexes. *Coord. Chem. Rev.* **2005**, 249, 633-662.
- (47) Lu, T.; Chen, F. Multiwfn: a multifunctional wavefunction analyzer. *J. Comput. Chem.* **2012**, 33, 580-92.
- (48) Frisch, M. J.; Trucks, G. W.; Schlegel, H. B.; Scuseria, G. E.; Robb, M. A.; Cheeseman, J. R.; Scalmani, G.; Barone, V.; Mennucci, B.; Petersson, G. A.; Nakatsuji, H.; Caricato, M.; Li, X.; Hratchian, H. P.; Izmaylov, A. F.; Bloino, J.; Zheng, G.; Sonnenberg, J. L.; Hada, M.; Ehara, M.; Toyota, K.; Fukuda, R.; Hasegawa, J.; Ishida, M.; Nakajima, T.; Honda, Y.; Kitao, O.; Nakai, H.; Vreven, T.; Montgomery, J. A.; Peralta, J. E.; Ogliaro, F.; Bearpark, M.; Heyd, J. J.; Brothers, E.; Kudin, K. N.; Staroverov, V. N.; Kobayashi, R.; Normand, J.; Raghavachari, K.; Rendell, A.; Burant, J. C.; Iyengar, S. S.; Tomasi, J.; Cossi, M.; Rega, N.; Millam, N. J.; Klene, M.; Knox, J. E.; Cross, J. B.; Bakken, V.; Adamo, C.; Jaramillo, J.; Gomperts, R.; Stratmann, R. E.; Yazyev, O.; Austin, A. J.; Cammi, R.; Pomelli, C.; Ochterski, J. W.; Martin, R. L.; Morokuma, K.; Zakrzewski, V. G.; Voth, G. A.; Salvador, P.; Dannenberg, J. J.; Dapprich, S.; Daniels, A. D.; Farkas, O.; Foresman, J. B.; Ortiz, J. V.; Cioslowski, J.; Fox, D. J. Gaussian 09, Revision D.01, Gaussian, Inc., Wallingford CT. **2009**.
- (49) Blanco, M. A.; Pendas, A. M.; Francisco, E. Interacting quantum atoms: A correlated energy decomposition scheme based on the Quantum Theory of Atoms in Molecules. *J. Chem. Theory. Comput.* **2005**, 1, 1096-1109.
- (50) te Velde, G.; Bickelhaupt, F. M.; Baerends, E. J.; Guerra, C. F.; Van Gisbergen, S. J. A.; Snijders, J. G.; Ziegler, T. Chemistry with ADF. *J. Comput. Chem.* **2001**, 22, 931-967.
- (51) Pyykko, P. Additive Covalent Radii for Single-, Double-, and Triple-Bonded Molecules and Tetrahedrally Bonded Crystals: A Summary. *J. Phys. Chem. A* **2015**, 119, 2326-2337.
- (52) Reed, A. E.; Weinstock, R. B.; Weinhold, F. Natural population analysis. *J. Chem. Phys.* **1985**, 83, 735-746.
- (53) Leyva-Parra, L.; Diego, L.; Yanez, O.; Inostroza, D.; Barroso, J.; Vasquez-Espinal, A.; Merino, G.; Tiznado, W. Planar Hexacoordinate Carbons: Half Covalent, Half Ionic. *Angew. Chem., Int. Ed.* **2021**, 60, 8700-8704.

- (54) Muller, P. Glossary of terms used in physical organic chemistry (IUPAC Recommendations 1994). *Pure Appl. Chem.* **1994**, 66, 1077–1184.